Open Access

Recent Progress in Materials

LIDSEN Publishing Inc.

Original Research

Assessment of Mineral Gain in White Spot Lesions Using CPP-ACP and CPP-ACFP in Different Clinical Protocols: A Proof of Concept Study

Carol Tran [1, †, ‡], Laurence J. Walsh [2, †, *]

School of Dentistry, The University of Queensland, Herston QLD 4006, Australia; E-Mails: c.tran@cqu.edu.au; l.walsh@uq.edu.au

‡ Current Affiliation: Central Queensland University, Rockhampton QLD 4740, Australia

† These authors contributed equally to this work.

* **Correspondence:** Laurence J. Walsh; E-Mail: l.walsh@uq.edu.au

Academic Editor: Eugeniusz Sajewicz

Special Issue: Advanced Dental Materials

Recent Progress in Materials
2021, volume 3, issue 4
doi:10.21926/rpm.2104046

Received: September 28, 2021
Accepted: November 23, 2021
Published: November 26, 2021

Abstract

Subsurface remineralization can be promoted by the topical application of nanoparticles of casein phosphopeptide-amorphous calcium phosphate (CPP-ACP). To assess changes in enamel white spot lesions, an in situ proof-of-concept investigation was performed using 5 subjects (all of whom were healthy young adults) with a cross-over study design. Custom orthodontic brackets were attached to the buccal surfaces of the maxillary second premolar and first molar teeth. Each bracket had a recess that held a slab of enamel with a standardized 100 µm deep white spot lesion (WSL). Changes in mineral were evaluated in lesion cross sections using backscatter electron imaging (BSE) and electron probe microanalysis (EPMA). The following products were applied twice daily for 2 weeks: GC Tooth Mousse™ (CPP-ACP), Tooth Mousse Plus™ (CPP-ACFP), CPP-ACFP Mineral Enhanced (CPP-ACFP Enh), or the vehicle paste of CPP-ACFP containing 900 ppm fluoride. To ensure blinding, all products had identical flavours and packaging. For each subject, the products were used in a random sequence, with

washout periods between products. Compared to the baseline situation, favourable changes in white spot lesions occurred with all products. Analysis of enamel samples in cross section showed improvements in mineral levels, as seen in BSE grey scale levels from the enamel surface through the lesion. These were accompanied by enhanced calcium and phosphorus levels as seen using EPMA. The ranking of products for subsurface mineral gain, from best to worst, was: CPP-ACFP = CPP-ACFP Enh > CPP-ACP > vehicle with fluoride. Rapid remineralization occurred in this clinical model, which is due to a combination of factors: the enamel slabs were located on tooth surfaces exposed to parotid saliva, the surfaces were brushed regularly to remove dental plaque biofilm, and compliance with twice daily topical use of products was high. Such model systems may be useful for screening new product formulations for their effect on enamel WSL.

Keywords
Casein phosphopeptide-amorphous calcium phosphate; remineralization; mineral gain; in situ model; white spot lesion; EPMA

1. Introduction

In dental practice, the use of topical products containing nanoparticles of casein phosphopeptide-amorphous calcium phosphate (CPP-ACP) or casein phosphopeptide-amorphous calcium fluoride phosphate (CPP-ACFP), such as Tooth Mousse™/ MI Paste™ and Tooth Mousse Plus™/ MI Paste Plus™ (GC Corp, Tokyo, Japan) has been shown to provide a range of clinical benefits, including arrest and regression of enamel white spot carious lesions (WSL) [1-4]. This has been supported by numerous systematic reviews [5-12]. As a naturally derived remineralizing technology, CPP-ACP is a partner to fluoride, providing the bioavailable calcium and phosphate ions required for remineralization. Many contemporary uses of CPP-ACP incorporate fluorides of various types. CPP can bind and stabilize fluoride ions, delivering them in the ideal stoichiometric ratio (5:3:1 for calcium: phosphate: fluoride) [2].

A particular area of interest has been the use of CPP-ACP during treatment with fixed orthodontic appliances [13-19], as this is a time of higher caries risk [20]. As well as acting as a remineralizing agent, CPP-ACP can also influence the dental plaque microflora to lower the levels of key pathogens [21, 22], by acting as a prebiotic agent [23-29]. This biological influence adds to the ability of these nanoparticles to deliver bioavailable calcium, phosphate, and fluoride, to cause mineral gain in the subsurface regions of enamel WSL [2, 3].

Past human in situ clinical studies of CPP-ACP have used a range of delivery systems for this material, including gums and lozenges, dentifrices, or as a topical crème, with the agent being applied directly to enamel slabs located on the palatal surfaces of removable appliances. When removable appliances are used, the enamel slabs are retrieved for later assessment of mineral changes in WSL by using transverse microradiography [30-34]. A limitation of using removable appliances to hold enamel slabs is that these appliances are removed before eating and drinking, and before toothbrushing or other oral hygiene procedures. Likewise, when wearing such appliances, participants have been instructed not to eat or drink anything except water. In these

studies, the appliances were cleaned using distilled water rather than a dentifrice. Hence, the dental plaque biofilm over the lesions remains largely undisturbed. Access of enamel lesions to saliva will also differ in the removable appliance model from the normal situation because of the location of the slabs somewhat away from the dental arch. Regional differences in salivary flow and in the composition and behaviour of the salivary film will affect the likelihood of ions from the saliva contributing to remineralization [35, 36]. Such factors may explain why the extent of mineral gain over time in such lesions may well be slower than may be seen in everyday clinical practice.

Topical products containing CPP-ACP are typically applied to the teeth immediately after toothbrushing. At this time, most visible deposits of dental plaque biofilm should have been removed from the surface of the WSL. This application protocol also allows the product to interact with the stimulated saliva elicited by the toothbrushing intervention, and with fluoride ions from a fluoride dentifrice. Because of this, one could expect greater or more rapid remineralization.

Such thought processes have led to studies where enamel slabs with WSL were directly bonded to the buccal surfaces of maxillary first or second molars. In 2015, Peric *et al*. used this approach in patients with Sjogren's syndrome, and showed using scanning electron microscopy (SEM) that twice daily application of CPP-ACP or CPP-ACFP crème after toothbrushing over 28 days caused the partial or complete occlusion of surface defects in the enamel lesions, which contributed to a more flattened appearance of the enamel surface [37]. They also assessed the surface composition using energy dispersive spectroscopy (EDS), but did not find changes in atomic ratios.

Later work by Ferrazzano *et al.* in 2011 [38] used SEM to assess changes in the surface topography of the enamel following application of CPP-ACP. They showed that the topical application of a CPP-ACP crème thrice daily for one month onto enamel slabs with WSL bonded to the buccal surfaces of maxillary first molars in healthy subjects aged from 10 to 16 years created a homogenous coating of mineral. They also pointed out that the advantages from this type of experimental model include a more realistic clinical situation because of exposure to the diet and to saliva, with regular oral hygiene measures still able to be performed. At the same time, additional compliance requirements around removing an appliance are removed [38].

As both of the previous studies had examined the surface features of WSL treated with CPP-ACP, it was of interest to use an in situ model to explore the effects of different CPP-ACP formulations on the subsurface, by examining enamel lesions in cross-section, to assess mineral density and elemental composition through the treated WSL. As a further refinement of the in situ model, enamel slabs with standardized WSL with a depth of 100 µm were not bonded to the teeth directly, but rather were placed without using adhesives into bonded custom-made orthodontic brackets attached to the teeth. This allowed the same site to be used for different enamel slabs, with each slab exposed to a different treatment agent. As well, the present study assessed mineral gain from cross-sections of the treated lesions by using backscatter electron imaging (BSE) to measure mineral density [39], and electron probe microanalysis (EPMA) to determine composition [40-42].

2. Materials and Methods

2.1 Enamel Slabs and WSL Creation

This proof-of-concept study followed a double-blinded, randomized, controlled crossover design. Changes in the enamel WSL were tracked with a 2 week period of use for different CPP-ACP products.

The overall design of the study was based on previous work using enamel slabs [33, 34]. All products had identical flavour and consistency, and the subjects were blinded to their use by using coded tubes. Likewise, analysis of samples was blinded. The project was approved by the institutional human ethics committee (Approval 2010000646).

A total of 58 extracted sound premolars which had been extracted for orthodontic reasons from teenage individuals residing in a community without community water fluoridation were selected. The teeth were gamma irradiated (25 kGy) and then stored in 0.1% thymol solution to maintain hydration. All teeth were inspected under a microscope at 20X to exclude any samples where the enamel surfaces showed fluorosis, hypomineralization, or physical defects such as microcracks or existing white spot lesions. The naturally flat areas on the buccal and lingual surfaces were used to prepare enamel slabs. Prior to commencing this process, a 3 x 4 mm window was created on each tooth with acid resistant nail varnish. The tooth was then immersed for 7 days at 37°C in 40 mL of a pH 4.5 demineralizing solution containing 2.2 mM Ca^{2+}, 2.2 mM PO_4^{3-} and 0.05 M acetic acid. This protocol has been used previously to create consistent visible white spot lesions of 100 µm in depth [39]. The varnish was then removed with acetone. A low speed diamond saw (Isomet, Buehler, Lake Bluff, IL, USA) was used to prepare 100 enamel slabs of 1 x 2 x 1 mm. These were then stored in a 100% humid environment until used. Baseline measurements were made from these samples. The slabs were allocated randomly to the subjects, so that they could be placed into the bracket for one of the phases of active treatment.

2.2 Clinical Protocol

A total of 5 healthy adult fully dentate subjects, all of whom were dental students or dental scientists, were involved in the study (age range 20-28 years, 3 males and 2 females). The minimum number of subjects was chosen as 5, based on the cross-over design being used. This sample size was in keeping with past studies of CPP-ACP using in situ models with crossover designs [33].

All subjects provided informed consent. None had significant medical conditions or were on medications which could influence salivary flow. All participants were in a state of oral health, with an absence of caries, periodontal disease or other oral pathology. Clinical examination indicated no untreated dental caries, no active carious lesions, and a good standard of plaque control. All subjects had normal salivary gland function, with unstimulated whole salivary flow rates equal to or greater than 0.25 mL/min and paraffin stimulated whole salivary flow rates of at least 1.0 mL/min.

The manufacturer (GC Corp., Tokyo, Japan) supplied the test products in identical and nondescript packaging and containers, with numerical codes. Products were assigned to each active test period in a random manner, with neither investigators nor subjects being aware of the contents. All subjects applied the test products twice daily immediately after brushing (i.e. in the morning at ~7.00 AM and in the evening at ~9.00 PM). Toothbrushing was undertaken with a supplied non-fluoride dentifrice (Snappy Jaws - strawberry flavour, Herbal Wisdom Natural Foods, Bangalow, NSW, Australia). The subjects followed their normal diet and performed their customary oral hygiene procedures throughout the study. No other fluoride products or remineralizing agents were used.

After applying 0.5 mL of the test product onto the brackets using a finger, subjects were required to spit out the excess, and then refrain from eating or drinking for 30 minutes. This was done to ensure optimal contact of the product with the enamel slabs. Otherwise, subjects were allowed to

eat and drink as normal. The enamel slabs were located in custom made orthodontic brackets with buccal recesses, which had been fabricated using CAD-CAM methods (Figure 1). The brackets were bonded to the buccal aspect of the left maxillary premolar and molar teeth (25 and 26) (Figure 1). This region is easy to clean by toothbrushing. and has ready access to stimulated saliva due to its proximity to the parotid papilla. The tooth surfaces were acid etched and a resin bonding agent (Unite ™ bonding adhesive, 3M Unitek, Monrovia, CA, USA) used to attach the brackets, in line with the manufacturer's instructions. The brackets remained in place for the duration of the study, with the slabs being changed for each treatment cycle.

Figure 1 Left: Custom-made brackets, showing the patterned side (used for bonding) and the opposite side with a recess for holding the slabs. The scale bar on the left is in mm. Right: A clinical image showing brackets attached to maxillary premolar and molar teeth (25 and 26). Each bracket recess holds one enamel slab located within Cavit.

The enamel slabs were held in place within the recess in the brackets with a water-setting rigid gypsum-based material (Cavit™, 3M-Espe, Neuss, Germany) designed for use as a temporary dressing of endodontic access forms. This material was preferred over composite resin and glass ionomer cement, because of greater ease of removal and to avoid halo effects from ion release, respectively.

After placing the brackets onto the buccal surfaces of the premolar and molar teeth, a 2 week acclimatization period followed, before commencing use of the products. Each subject used the products in a random sequence. The treatments were a 10% CPP-ACP crème (GC Tooth Mousse), a 10% CPP-ACFP crème containing 900 ppm fluoride (GC Tooth Mousse Plus), the same ACFP crème with 0.1% calcium chloride added (CPP-ACFP Enh), and a control vehicle that contained the same level of fluoride (900 ppm) but lacked the CPP-ACP or CPP-ACFP active ingredient.

There were 10 X 14-day periods including alternating phases of passive washout followed by use of the active product. The 14-day washout period was intended to minimize the influence of previous product exposure. At the start of each phase, a thorough prophylaxis with a non-fluoride prophylaxis paste was undertaken, with the issue of a new manual toothbrush and supplies of the standard non-fluoride dentifrice. Specific instructions regarding product use were reinforced. A new enamel slab was then placed in the brackets, and these were then removed at the end of that particular phase.

At the completion of each phase, the slabs were collected. Untreated WSL baseline samples and slabs retrieved from orthodontic brackets were embedded in epoxy resin in 25 mm mounts to give

a cross section of the slab. The surface of the embedded samples was polished using 3 and 1 µm diamond polishing pastes, and then with a 0.25 µm aluminium oxide polishing paste, so that they were optically smooth. The samples were then coated with a 20 nm layer of carbon.

Samples with damaged surfaces were excluded from the analysis. Likewise, any enamel samples which dislodged prematurely from the brackets during a treatment phase were excluded from further analysis. Because of logistical requirements during sample embedding and polishing, it was not possible to track the slabs for individual patients, and thus data were pooled for treatment groups, with a final sample size of 10.

2.3 Sample Analysis

To assess mineral levels, backscatter electron microscopy of enamel slab cross sections was used, as described in detail previously, with analysis of grey scale changes across the lesion using Adobe Photoshop™ CS2 software [39]. BSE has been shown previously to give good estimates of enamel mineral density [42, 43]. An 8 bit grey scale was used (with 0 representing black and 255 representing white). In the present study, normal healthy enamel had a consistent grey scale value of 93 $\pm$ 3. Lower grey scale values than this indicate mineral loss.

For BSE, samples were examined in a JOEL JXA-8200 Superprobe Electron Probe Microanalyzer (Akishima, Tokyo, Japan), at an accelerating voltage of 20 kV in backscatter mode. The same instrument was also used for EPMA. SEM backscatter imaging at low magnification (50X) was used to identify the areas of interest, which were then imaged in backscatter mode at a final magnification of 150X. Digital images (1024 X768 pixels) were recorded of the WSL regions. Image J software (version 1.47, US National Institutes of Health) was used to plot grey scale changes across the depth of the sample in cross section, to a depth of 200 µm from the surface. Scale calibration bars in the SEM images were used to calibrate the Image J software so that all dimensions were expressed in micrometres. A selection area of 20 µm wide and 200 µm deep positioned at right angles to the enamel surface was used for data collection. The analysis function was used to collect average values at each 1.5 µm depth interval. The data for grey scale were then exported to a spreadsheet for statistical analysis. Data sets were checked for normality and then analyzed using one-way ANOVA, with Tukey-Kramer post-tests.

As the WSL lesion depth was around 100 µm, the analysis focussed on changes in that region, since there was normal enamel from 100 µm onwards. To gain a pictorial representation of the subsurface features according to grey scale, the surface plot tool of Image J software was used. Standardized plots of grey scale changes over a depth of 150 µm were subjected to analysis. Adobe Photoshop™ CS2 software was used to measure the pixel area of subsurface lesions. Data were then pooled to give a final N of 10 for each lesion. Data sets were checked for normality and then analyzed using one-way ANOVA with Tukey-Kramer post-tests.

EPMA was undertaken using methods described in detail previously [40, 41]. In brief, the excitation voltage was 15 kV and the current was 20 mA. Two diffracting spectrometers were assigned to collect information for calcium and phosphorus simultaneously. Spot analysis was performed at 10 µm intervals along a transverse line perpendicular to the outer surface to a depth of 200 µm. A set of 3 lines was performed for each sample. The diameter of the electron beam was 2 µm, and the counting time was 10 sec at each point. Wilberforce fluorapatite was used as a

standard, and the PAP modified version of the ZAF software package (Cameca, Corbevoie, France) was used for data correction. Final values of atomic composition in weight percent were calculated.

3. Results

3.1 Qualitative Findings

BSE imaging showed clear differences between the treatments (Figure 2). At baseline, the white spot lesions had intact surfaces overlying subsurface areas of mineral loss, which extended to a typical depth of 100 µm. As remineralization occurred with fluoride, the signal at the surface increased dramatically and lesion size reduced. The changes with CPP-ACP products were seen across the extent of white spot lesion, with almost complete disappearance of the lesion in the two products which contained CPP-ACP and fluoride. On a qualitative basis, the extent of change in the subsurface was rated, from most to least, as follows: CPP-ACFP = CPP-ACFP Enh > CPP-ACP > fluoride vehicle.

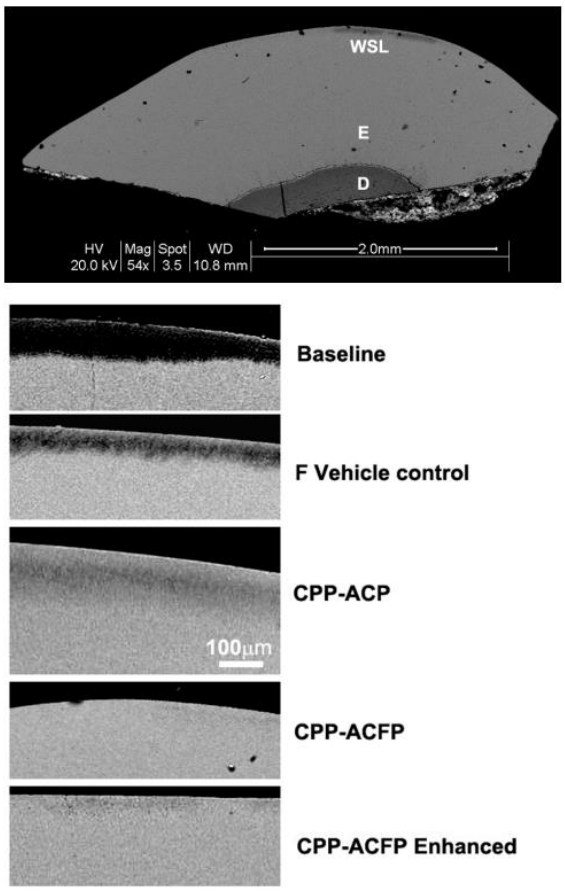

Figure 2 Upper panel: A typical enamel slab at baseline, showing the white spot lesion (WSL), and the underlying enamel (E) and dentine (D). The scale bar shows 2 mm. Bottom panel: Backscatter images of typical enamel slabs in cross section, following treatment in situ for 2 weeks twice daily. All images are at the same final magnification. The scale bar indicates 100 µm. At baseline, the initial white spot lesions were around 100 µm in depth. This lesion depth can also be seen in 2D and 3D in Figure 3 and Figure 4.

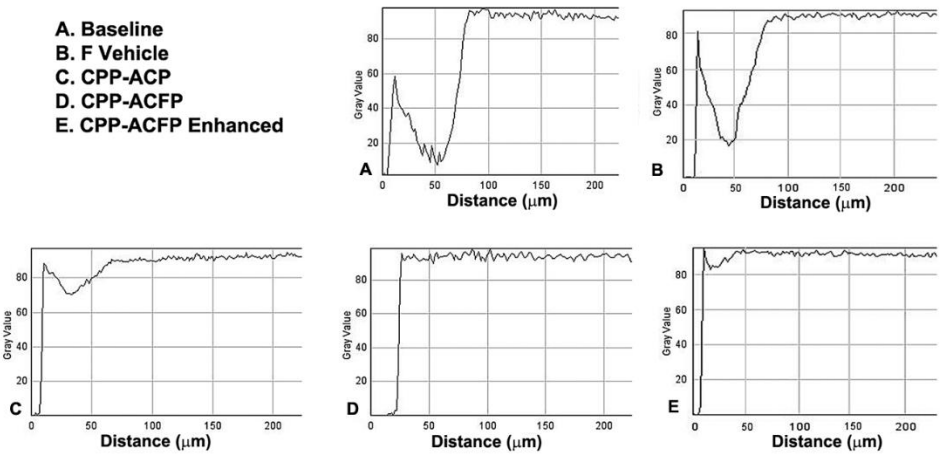

Figure 3 2 D Cross sectional plots of grey scale density versus depth in representative samples, based on a single sampling frame 20 µm wide. The vertical axis is grey scale values. Sound enamel is 93 on this scale. The depth of the lesion at baseline was a distance of 100 µm.

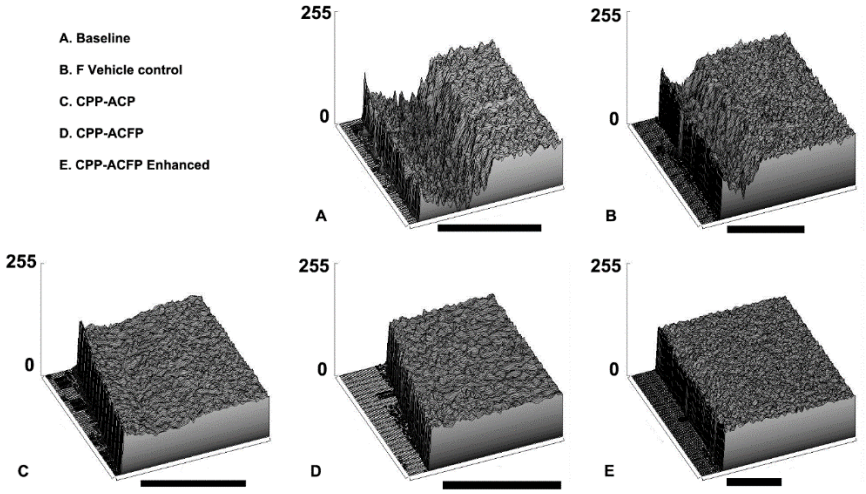

Figure 4 3 D mineral density plots showing grey scale values across the subsurface region of 5 slabs, with the enamel surface positioned on the left. The vertical axis is grey scale values, with sound enamel being 93. The scale bar in each image represents 100 µm. These images provide the 3D information for same samples as the 2D plots in Figure 3 above.

3.2 Quantitative Findings

In terms of mineral gain, as evidenced by elevated grey scale scores and a reduction in lesion size, there was a significant difference between the treatments, and between the treatments and the baseline. Plots of grey scale versus depth showed the characteristic appearance for WSL at baseline (Figure 3 A). Lesion area reduced with CPP-ACP treatment, and even more so with CPP-ACFP (Figure 3 B-E). Plots of grey scale versus distance (Figure 4) demonstrated how the subsurface changes

occurred with the various treatments. The ranking between products was, once again, CPP-ACFP = APP-ACFP Enhanced > CPP-ACP > fluoride vehicle.

Assessing the area of the subsurface lesion and comparing this with the situation at baseline (Figure 5), there was a small reduction in lesion size from the vehicle containing fluoride versus the baseline ($P < 0.05$), with an even greater benefit from CPP-ACP, which was superior to the vehicle alone ($P < 0.05$) and improved from the baseline ($P < 0.001$). The greatest benefit compared to the vehicle and to the baseline was seen with CPP-ACFP in both its versions (all $P < 0.001$), however according to the lesion area analysis, differences between the two CPP-ACFP products were not statistically significant (Figure 6).

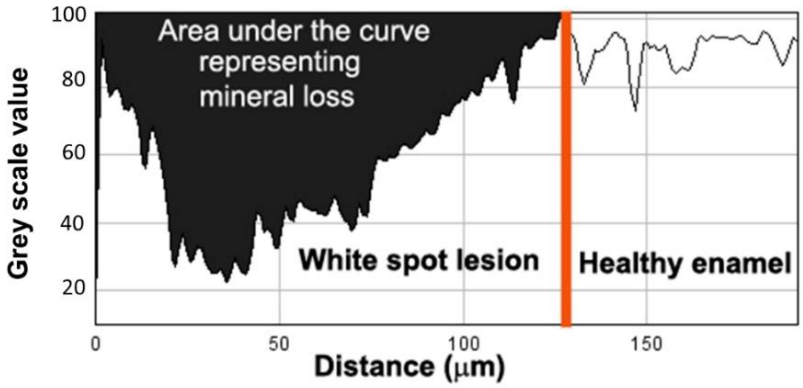

Figure 5 A plot of mineral density (grey scale value) versus distance across the cross section of a white spot lesion at baseline, showing in black where mineral has been lost from the subsurface. The red line indicates the maximum depth of the lesion at this point (In this example, 125 µm). The red line marks the boundary between the lesion and the deeper normal enamel. The grey scale value for normal healthy enamel is 93.

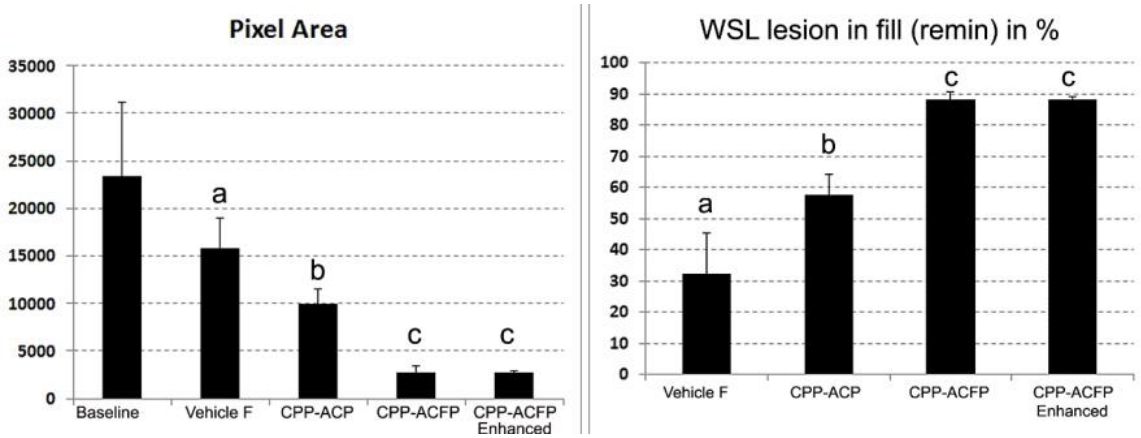

Figure 6 Left: Pixel areas for subsurface lesions (the area under the curve). Lower case letters show groups that were significantly different from the baseline and from one another, by Tukey-Kramer post-hoc tests after ANOVA. Bars show means and standard deviations. Right: Calculated lesion in fill by remineralization based on the pixel area change from WSL at baseline. Lower case letters show groups that were significantly different from one another.

3.3 Grey Scale Analysis

When sampling frames of 200 X 100 µm were used to assess all pixels in the frame for grey scale value using the histogram function of Adobe Photoshop (Figure 7), the same overall trends were seen, with the highest grey scale values (and hence the greatest mineral) being found in healthy enamel. This was not significantly different from enamel that had been remineralized using CPP-ACPF or the enhanced version of CPP-ACPF (Figure 8). The overall ranking for mineral levels based on pixel grey scale values was CPP-ACFP = CPP-ACFP Enh = normal enamel (beneath the WSL) > CPP-ACP > fluoride vehicle > WSL at baseline.

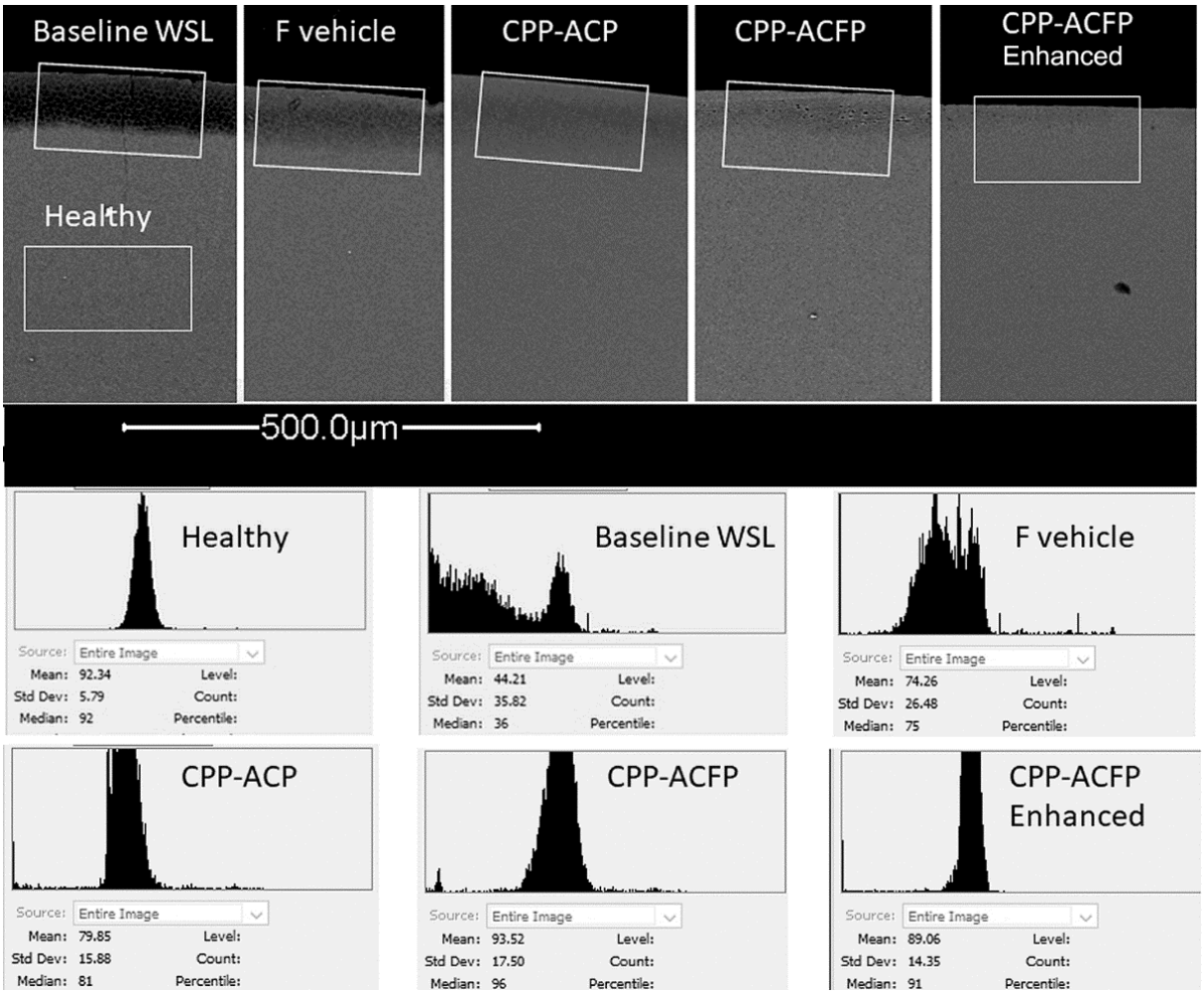

Figure 7 Analysis of the distribution of pixel grey scale values in lesion cross sections in the sampling frames shown by the rectangles. As mineral levels rise, the distribution shown on the histogram plots moves to the right, towards the value of 93 for normal enamel.

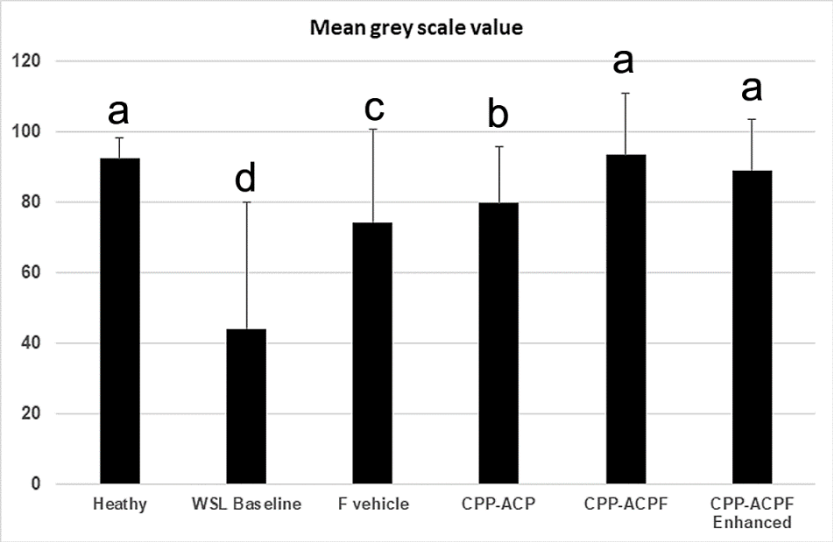

Figure 8 Statistical differences between sample groups for mean grey scale pixel values. Lower case letters show groups that were significantly different from one another by Tukey-Kramer post-hoc tests after ANOVA. The sample size for N in each group was 84,000 pixels.

3.4 EPMA

In the WSL at baseline, there was a marked reduction in calcium and phosphorus content in the body of the lesion (Figure 9), in exactly the same pattern as noted on the grey scale plots. The fluoride vehicle caused a small gain in calcium and phosphorus that was superficial. A marked level of improvement in subsurface calcium and phosphorus occurred with CPP-ACP. The levels of calcium and phosphorus achieved for CPP-ACFP and the mineral enhanced version of CPP-ACP were identical to those for sound enamel. Surface levels of fluorine were increased with all treatments, with the largest improvement occurring for the CPP-ACFP mineral enhanced product.

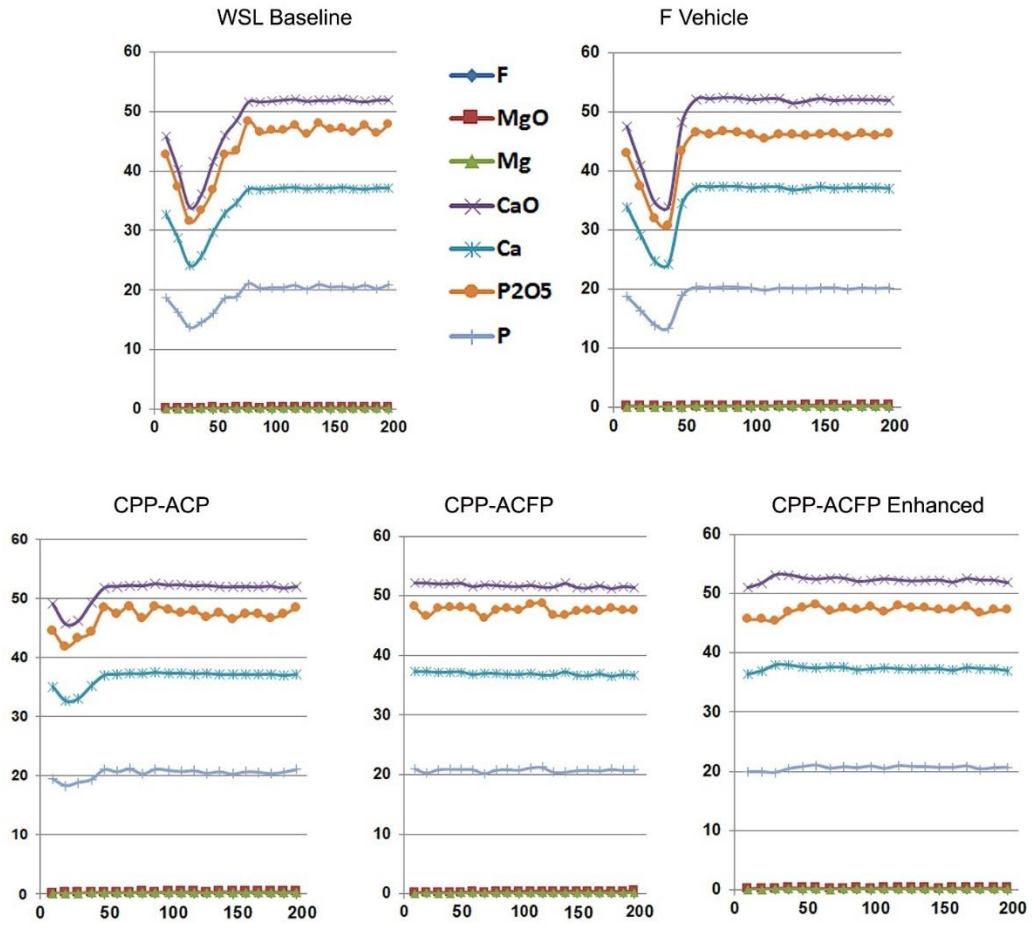

Figure 9 EPMA results arranged according to the treatment group, showing proportions in weight percent on the vertical scale, versus distance from the enamel surface on the horizontal scale. Data show mean values for N = 15 points at each sample location. The initial WSL at baseline had a depth of ~100 µm. Treatment with CPP-ACFP restores the profile of the treated area to that of normal enamel.

4. Discussion

This study reveals some interesting differences between the fluoride vehicle control and various CPP-ACP-based products in terms of subsurface changes in WSL. Overall, the pattern of greater mineral gain than fluoride alone with CPP-ACP, and greater effects for CPP-ACP combined with fluoride is consistent with previous in situ studies in which enamel slabs were embedded into removable acrylic appliances and were located on the hard palate [33, 34]. The ability to explore grey scale values in a cross-section of the enamel provides an insight into the way that mineral and water are organized in a white spot lesion, with regular variations in mineral density showing the structure of the enamel rods. As subsurface mineral gain occurs, the regular pattern of the enamel microstructure disappears to a more even platform of dense mineral. This aspect is best shown in the 3D plots (Figure 4). A similar pattern of results was seen with all the methods of analysis used for the lesion cross sections, with the EPMA data showing superior mineral gain in the subsurface

for CPP-ACFP over CPP-ACP, and the treated enamel WSL achieving mineral levels the same as normal health enamel.

The present study reinforces the potential for BSE imaging to reveal changes in mineral in enamel. This approach has been used previously to assess the extent by which different materials can exert tooth surface protection, when used around orthodontic brackets to prevent decalcification of enamel [39]. The grey scale profiles from BSE imaging correlated well with the compositional plots for calcium and phosphorus from EPMA. Both approaches provided a trend across the various products which is similar to that reported for mineral density by transverse microradiography, and for microhardness [33, 34]. The consistent feature of such profiles is a predominantly surface effect for fluoride alone, but an effect which extends across the WSL when CPP-ACP is present, either alone or together with fluoride. The EPMA data also show that the CPP-ACP treatments dramatically elevated levels of fluorine in the enamel and particularly in the outermost 25 µm of the enamel, a point which aligns with past studies of the acid resistance of enamel which has been remineralized by CPP-ACP, either alone or in combination with fluoride [32].

While there are benefits in an experimental model where samples are attached to the teeth, either directly [37, 38] or through brackets (as in the present investigation), this approach does come with the risk of dislodgement or damage from toothbrushing. There is also the possibility that the adhesives or other materials used to retain the enamel slabs could influence the remineralization process. In the present study, a low solubility gypsum-based material (Cavit ™) was used. This may have made a small contribution to the level of calcium ions in the local environment, but any such effect would have been the same for all the products being compared. In the same manner, should an in situ system with brackets be chosen, glass ionomer cement should not be used to bond the brackets to the teeth, or to fix the enamel slabs in place, since this will have a significant effect on the sample through the release of fluoride, not only initially, but over time through successive cycles of release followed by recharging from fluoride from dentifrices or other products [44].

The EPMA analysis used in the present study showed subtle differences between the enhanced and non-enhanced versions of Tooth Mousse Plus, which were not readily apparent from the BSE grey scale plots. The higher levels of fluorine and the higher calcium to phosphate ratios seen in the outer regions of the enamel surface suggest that this mineral dense layer has a higher proportion of fluorapatite which should endow it with greater acid resistance than surrounding normal enamel. This point needs to be examined further using acid challenge experiments, with SEM examination of the surface or an assessment of changes in enamel microhardness before and after acid challenge.

Finally, the use of mineral density data to generate 3-dimensional plots is a novel approach for assessing remineralization of the body zone of white spot lesions. The current findings extend those of earlier investigations in which treated WSL lesions were examined using SEM. These showed that voids between enamel prisms on the surface had been filled in by deposits of mineral when CPP-ACP was used [37, 38, 45]. The present study showed mineral gain below the surface, in the body of the lesion. The ability to achieve mineral deposition deep within WSL is a unique characteristic of CPP-ACP, and explains why it can cause visible regression of WSL so effectively [3, 5].

The in situ model used in the present study builds on the benefits of using a more realistic model system for assessing remineralization that have been discussed in earlier work [38]. Twice daily brushing will reduce biofilm on the slabs and maximize the opportunity for products to contact the surface, and maximize the benefits from exposure to parotoid saliva. This combination of factors

provides a suitable situation for remineralization of the subsurface of the lesions to occur, especially in young healthy patients with normal salivary flow. Remineralization of the surface has been shown in past studies of enamel slabs bonded to maxillary posterior teeth, both in healthy young patients [38] and in older adult patients with Sjogren's syndrome [37]. Past studies showed closure of surface porosities, while the present study using lesion cross-sections showed subsurface mineral gain. Taken together, these findings emphasize the effectiveness of remineralization protocols using CPP-ACP, in an experimental model with a high level of realism.

Finally, a key point in the present study, all subjects were dentally aware and had high compliance, since all were dental undergraduate or postgraduate students. Patients with low compliance, poor oral hygiene or compromised salivary parameters would not show such rapid changes in white spot lesions as those documented in the present study.

5. Conclusions

This proof-of-concept study shows that rapid remineralization of enamel WSL can occur when there is ready access to parotid saliva, regular brushing of enamel surfaces, and twice daily topical use of CPP-ACP or CPP-ACFP products by highly compliant healthy subjects. Based on mineral density assessments of lesion cross sections (using BSE) and EPMA assessments of calcium and phosphorus levels, CPP-ACP was superior to fluoride for mineral gain in the subsurface region of WSL, and CPP-ACFP was superior to CPP-ACP. In situ model systems may have value for screening new product formulations for their effect on mineral gain in the subsurface region of enamel WSL.

Acknowledgments

We thank Dr Lei Chai and Professor Hein Ngo for their assistance and advice respectively with EPMA analysis, and Drs Harry Akers and Jason Yap for coordination of the clinical appointments. We also thank Professor Bennett T. Amaechi for assistance with orthodontic bracket fabrication, and the UQ School of Earth Sciences for assistance with sample mounting and polishing.

Author Contributions

The study was conceived by both authors. Dr Tran prepared the enamel slabs and performed the clinical components of the study. Dr Walsh undertook the image analysis and statistical comparisons, and supervised the EPMA assessments. Both authors contributed to writing the manuscript, and approved the final submission.

Funding

This study was supported by grants from the Australian Dental Research Foundation (ADRF) and the Cooperative Research Centre for Oral Health. An abstract arising from this project was published previously in an annual report of the ADRF [46].

Competing Interests

The authors declare that no competing interests exist.

References

1. Reynolds EC. Remineralization of enamel subsurface lesions by casein phosphopeptide-stabilized calcium phosphate solutions. J Dent Res. 1997; 76: 1587-1595.
2. Reynolds EC. Anticariogenic complexes of amorphous calcium phosphate stabilized by casein phosphopeptides: A review. Spec Care Dentist. 1998; 18: 8-16.
3. J Walsh L. Molecular and pharmaceutical aspects of novel methods and materials for the prevention of tooth structure loss. Curr Pharm Biotechnol. 2017; 18: 45-51.
4. Philip N. State of the art enamel remineralization systems: The next frontier in caries management. Caries Res. 2019; 53: 284-295.
5. Yengopal V, Mickenautsch S. Caries preventive effect of casein phosphopeptide-amorphous calcium phosphate (CPP-ACP): A meta-analysis. Acta Odontol Scand. 2009; 67: 321-332.
6. Bader JD. Casein phosphopeptide-amorphous calcium phosphate shows promise for preventing caries. Evid Based Dent. 2010; 11: 11-12.
7. Ekambaram M, Mohd Said SN, Yiu CK. A review of enamel remineralisation potential of calcium- and phosphate-based remineralisation systems. Oral Health Prev Dent. 2017; 15: 415-420.
8. Bijle MNA, Yiu CKY, Ekambaram M. Calcium-based caries preventive agents: A meta-evaluation of systematic reviews and meta-analysis. J Evid Based Dent Pract. 2018; 18: 203-217.
9. Wu L, Geng K, Gao Q. Early caries preventive effects of casein phosphopeptide-amorphous calcium phosphate (CPP-ACP) compared with conventional fluorides: A meta-analysis. Oral Health Prev Dent. 2019; 17: 495-503.
10. Tao S, Zhu Y, Yuan H, Tao S, Cheng Y, Li J, et al. Efficacy of fluorides and CPP-ACP vs fluorides monotherapy on early caries lesions: A systematic review and meta-analysis. PLoS ONE. 2018; 13: e0196660.
11. Asokan S, Geethapriya PR, Vijayasankari V. Effect of nonfluoridated remineralizing agents on initial enamel carious lesions: A systematic review. Indian J Dent Res. 2019; 30: 282-290.
12. Ma X, Lin X, Zhong T, Xie F. Evaluation of the efficacy of casein phosphopeptide-amorphous calcium phosphate on remineralization of white spot lesions in vitro and clinical research: A systematic review and meta-analysis. BMC Oral Health. 2019; 19: 295.
13. Sudjalim TR, Woods MG, Manton DJ, Reynolds EC. Prevention of demineralization around orthodontic brackets in vitro. Am J Orthod Dentofacial Orthop. 2007; 131: 705.e1-705.e9.
14. Wen-dan H, Ying-zhi L, Yuan-yuan X, Dong C. Study on application of CPP-ACP on tooth mineralization during orthodontic treatment with fixed appliance. Shanghai Kou Qiang Yi Xue. 2010; 19: 140-143.
15. Lopatiene K, Borisovaite M, Lapenaite E. Prevention and treatment of white spot lesions during and after treatment with fixed orthodontic appliances: A systematic literature review. J Oral Maxillofac Res. 2016; 7: e1.
16. Pithon MM, Baião FS, Sant'Anna LI, Tanaka OM, Cople-Maia L. Effectiveness of casein phosphopeptide-amorphous calcium phosphate-containing products in the prevention and treatment of white spot lesions in orthodontic patients: A systematic review. J Investig Clin Dent. 2019; 10: e12391.
17. Imani MM, Safaei M, Afnaniesfandabad A, Moradpoor H, Sadeghi M, Golshah A, et al. Efficacy of CPP-ACP and CPP-ACPF for prevention and remineralization of white spot lesions in

orthodontic patients: A systematic review of randomized controlled clinical trials. Acta Inform Med. 2019; 27: 199-204.

18. Bakdach WM, Hadad R. Effectiveness of different adjunctive interventions in the management of orthodontically induced white spot lesions: A systematic review of systematic reviews and meta-analyses. Dent Med Probl. 2020; 57: 305-325.
19. Sardana D, Manchanda S, Ekambaram M, Yang Y, McGrath CP, Yiu CK. Prevention of demineralization during multi-bracketed fixed orthodontic treatment: An overview of systematic reviews. Int J Paediatr Dent. 2021. Doi:10.1111/ipd.12927.
20. Walsh LJ, Healey DL. Prevention and caries risk management in teenage and orthodontic patients. Aust Dent J. 2019; 64: S37-S45.
21. Pukallus ML, Plonka KA, Holcombe TF, Barnett AG, Walsh LJ, Seow WK. A randomized controlled trial of a 10 percent CPP-ACP cream to reduce mutans streptococci colonization. Pediatr Dent. 2013; 35: 550-555.
22. Al-Batayneh OB, Al-Rai SA, Khader YS. Effect of CPP-ACP on Streptococcus mutans in saliva of high caries-risk preschool children: A randomized clinical trial. Eur Arch Paediatr Dent. 2020; 21: 339-346.
23. Philip NV, Walsh LJ. The potential ecological effects of casein phosphopeptide-amorphous calcium phosphate in dental caries prevention. Aust Dent J. 2019; 64: 66-71.
24. Philip N, Leishman SJ, Bandara HMHN, Walsh LJ. Casein phosphopeptide-amorphous calcium phosphate attenuates virulence and modulates microbial ecology of saliva-derived polymicrobial biofilms. Caries Res. 2019; 53: 643-649.
25. Fernando JR, Butler CA, Adams GG, Mitchell HL, Dashper SG, Escobar K, et al. The prebiotic effect of CPP-ACP sugar-free chewing gum. J Dent. 2019; 91: 103225.
26. Dashper SG, Shen P, Sim CP, Liu SW, Butler CA, Mitchell HL, et al. CPP-ACP promotes SnF_2 efficacy in a polymicrobial caries model. J Dent Res. 2019; 98: 218-224.
27. Philip N, Leishman SJ, Bandara HM, Healey DL, Walsh LJ. Randomized controlled study to evaluate microbial ecological effects of CPP-ACP and cranberry on dental plaque. JDR Clin Trans Res. 2020; 5: 118-126.
28. Widyarman AS, Udawatte NS, Theodorea CF, Apriani A, Richi M, Astoeti TE, et al. Casein phosphopeptide-amorphous calcium phosphate fluoride treatment enriches the symbiotic dental plaque microbiome in children. J Dent. 2021; 106: 103582.
29. Mao B, Xie Y, Yang H, Yu C, Ma P, You Z, et al. Casein phosphopeptide-amorphous calcium phosphate modified glass ionomer cement attenuates demineralization and modulates biofilm composition in dental caries. Dent Mater J. 2021; 40: 84-93.
30. Cai F, Shen P, Morgan MV, Reynolds EC. Remineralization of enamel subsurface lesions in situ by sugar-free lozenges containing casein phosphopeptide-amorphous calcium phosphate. Aust Dent J. 2003; 48: 240-243.
31. Cochrane NJ, Shen P, Byrne SJ, Walker GD, Adams GG, Yuan Y, et al. Remineralisation by chewing sugar-free gums in a randomised, controlled in situ trial including dietary intake and gauze to promote plaque formation. Caries Res. 2012; 46: 147-155.
32. Iijima Y, Cai F, Shen P, Walker G, Reynolds C, Reynolds EC. Acid resistance of enamel subsurface lesions remineralized by a sugar-free chewing gum containing casein phosphopeptideamorphous calcium phosphate. Caries Res. 2004; 38: 551-556.

33. Shen P, Cai F, Nowicki A, Vincent J, Reynolds EC. Remineralization of enamel subsurface lesions by sugar-free chewing gum containing casein phosphopeptide-amorphous calcium phosphate. J Dent Res. 2001; 80: 2066-2070.
34. Shen P, Manton DJ, Cochrane NJ, Walker GD, Yuan Y, Reynolds C, et al. Effect of added calcium phosphate on enamel remineralization by fluoride in a randomized controlled in situ trial. J Dent. 2011; 39: 518-525.
35. Dawes C, Watanabe S, Biglow-Lecomte P, Dibdin GH. Estimation of the velocity of the salivary film at some different locations in the mouth. J Dent Res. 1989; 68: 1479-1482.
36. Dawes C. Salivary flow patterns and the health of hard and soft oral tissues. J Am Dent Assoc. 2008; 139: 18S-24S.
37. Peric T, Markovic D, Petrovic B, Radojevic V, Todorovic T, Radicevic BA, et al. Efficacy of pastes containing CPP-ACP and CPP-ACFP in patients with Sjögren's syndrome. Clin Oral Invest. 2015; 19: 2153-2165.
38. Ferrazzano GF, Amato I, Cantile T, Sangianantoni G, Ingenito A. In vivo remineralising effect of GC Tooth Mousse on early dental enamel lesions: SEM analysis. Int Dent J. 2011; 61: 210-216.
39. Yap J, Walsh LJ, Naser-Ud Din S, Ngo H, Manton DJ. Evaluation of a novel approach in the prevention of white spot lesions around orthodontic brackets. Aust Dent J. 2014; 59: 70-80.
40. Ngo HC, Mount G, McIntyre J, Do L. An in vitro model for the study of chemical exchange between glass ionomer restorations and partially demineralized dentin using a minimally invasive restorative technique. J Dent. 2011; 39: S20-S26.
41. Knight GM, McIntyre JM, Craig GG, Mulyani. Electron probe microanalysis of ion exchange of selected elements between dentine and adhesive restorative materials. Aust Dent J. 2007; 52: 128-132.
42. Ngo H, Ruben J, Arends J, White D, Mount GJ, Peters MC, et al. Electron probe microanalysis and transverse microradiography studies of artificial lesions in enamel and dentin: A comparative study. Adv Dent Res. 1997; 11: 426-432.
43. Cochrane NJ, Iijima Y, Shen P, Yuan Y, Walker GD, Reynolds C, et al. Comparative study of the measurement of enamel demineralization and remineralization using transverse microradiography and electron probe microanalysis. Microsc Microanal. 2014; 20: 937-945.
44. Arbabzadeh-Zavareh F, Gibbs T, Meyers IA, Bouzari M, Mortazavi S, Walsh LJ. Recharge pattern of contemporary glass ionomer restoratives. Dent Res J. 2012; 9: 139-145.
45. Hua F, Yan J, Zhao S, Yang H, He H. In vitro remineralization of enamel white spot lesions with a carrier-based amorphous calcium phosphate delivery system. Clin Oral Investig. 2020; 24: 2079-2089.
46. Tran C, Chai L, Ngo H, Walsh LJ. Effects of tooth mousse plus on remineralization and fluoride uptake in artificially demineralized enamel: An in situ study using electron probe microanalysis. Aust Dent J. 2016; 61: S31.

Enjoy *Recent Progress in Materials* by:

1. Submitting a manuscript
2. Joining in volunteer reviewer bank
3. Joining Editorial Board
4. Guest editing a special issue

For more details, please visit:
http://www.lidsen.com/journals/rpm